Edge helicons and repulsion of fundamental edge magnetoplasmons in the quantum Hall regime

1999 J. Phys.: Condens. Matter 11 5143

(http://iopscience.iop.org/0953-8984/11/26/315)

J. Phys.: Condens. Matter **11** (1999) 5143–5156. Printed in the UK PII: S0953-8984(99)00321-5

Edge helicons and repulsion of fundamental edge magnetoplasmons in the quantum Hall regime

O G Balev†‡, P Vasilopoulos§ and Nelson Studart†

† Departmento de Física, Universidade Federal de São Carlos, 13565-905 São Carlos, Brazil
‡ Institute of Physics of Semiconductors, National Academy of Sciences, 45 Prospekt Nauky, Kiev 252650, Ukraine
§ Concordia University, Department of Physics, 1455 de Maisonneuve Boulevard O, Montréal, Canada, H3G 1M8

E-mail: vbalev@power.ufscar.br, takis@boltzmann.concordia.ca and studart@power.ufscar.br

Received 21 December 1998, in final form 14 April 1999

Abstract. A *quasi-microscopic* treatment of edge magnetoplasmons (EMPs) is presented for very low temperatures and confining potentials smooth on the scale of the magnetic length ℓ_0 but sufficiently steep at the edges that Landau-level (LL) flattening can be discarded. The profile of the unperturbed electron density is sharp and the dissipation taken into account arises only from electron intra-edge and intra-LL transitions due to scattering by acoustic phonons. For wide channels and filling factors $\nu = 1$ and 2, there exist independent EMP modes spatially symmetric and antisymmetric with respect to the edge. Some of these modes, named edge helicons, can propagate nearly undamped even when the dissipation is strong. Their density profile changes qualitatively during propagation and is given by a rotation of a complex vector function. For $\nu > 2$, the Coulomb coupling between the LLs leads to a repulsion of the uncoupled fundamental LL modes: the new modes have very different group velocities and are nearly undamped. The theory accounts well for the experimentally observed plateau structure of the delay times as well as for the spectral properties (phase and group velocities) of the EMPs and decay rates.

1. Introduction

Previous theoretical studies of edge magnetoplasmons (EMPs), the low-frequency collective excitations which propagate along the edges of a two-dimensional electron gas (2DEG) subject to a normal magnetic field $\boldsymbol{B}$, have indicated some important characteristics of EMPs, e.g., the gapless excitation spectrum, chirality [1] and the acoustic nature of the EMP [2]. However, the authors of references [1] and [2] have assumed density profiles which are infinitely sharp or smooth respectively and independent of the filling factor $\nu = n_0 h/|e|B$, where n_0 is the electron density in the bulk of the 2DEG. As a consequence, these profiles lack an essential quantum mechanical feature, the Landau-level (LL) structure. As was clearly shown in reference [3], and is reproduced in figure 1, the density profile for the cases of one and two occupied LLs, calculated by assuming a smooth parabolic confining potential at the edge, is quite different from those considered in the models of Volkov and Mikhailov [1] and Aleiner and Glazman [2]. Furthermore, the inadequacies of these models were clearly manifested in recent time-resolved magnetotransport experiments [4] that showed a plateau structure of the delay times reflecting the quantum Hall effect (QHE) plateaus and not accounted for in reference [2]. The experimental results also provided evidence of the essential role of the

0953-8984/99/265143+14$19.50

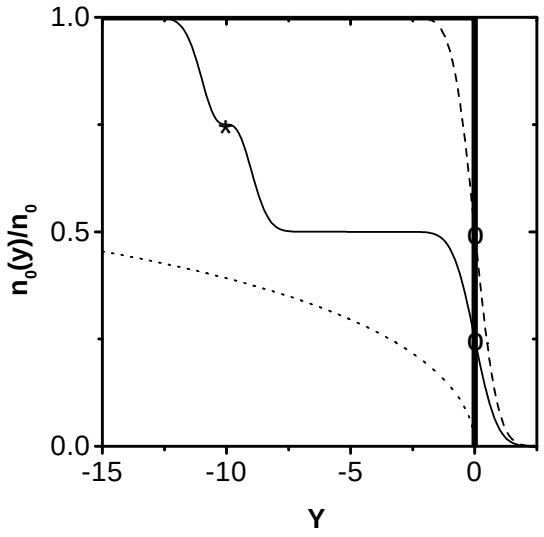

Figure 1. The unperturbed electron density $n_0(y)$, normalized to the bulk value n_0, as a function of Y. For the thick solid curves and the dotted curves, $Y = (y - y_{re})/\ell_0$, where y_{re} is the edge in the models of references [1] and [2]. The thick solid line is the density profile in the model of reference [1] and the dotted curve that of reference [2] for $n_0(y)/n_0 = (2/\pi)\arctan[(y_{re}-y)/a]^{1/2}$, and $a/\ell_0 = 20$. The dashed and solid curves show our calculated profiles for $\nu = 1, 2$ and $\nu = 4$, respectively. For the dashed and solid curves, $Y = (y - y_{r0})/\ell_0$; for the solid curve, $(y_{r0} - y_{r1})/\ell_0 = 10$. The star and open dots denote $n_0(y)/n_0$ at the edges of LLs: $n = 1$, y_{r1} or $Y = -10$; and $n = 0$, y_{r0} or $Y = 0$.

magnetic field dependence of the electronic structure at the edges. In addition, for a spatially homogeneous dissipation within the channel, the EMP damping was found to be quantized and independent of temperature [1] or it was treated phenomenologically [2]. The calculated damping rates [2] were strongly overestimated as compared with the experimental results [4]. These deviations are attributed to the inadequacy of the classical edge-wave mechanism, which in effect is employed by the theories of references [1] and [2], as regards describing the real edge-wave mechanism for the QHE regime found in the semiconductor heterostructures [4]. Notice that the classical edge-wave mechanism of the conventional EMPs [1,2] is the magnetic analogue of the Kelvin wave [5] at the edge of a rotating 'shallow' sea, with chirality determined by the Coriolis parameter [3]. For the classical edge-wave mechanism, the position of the edge does not vary but the charge-density profile at the edge does. Other drawbacks and the limited validity of the treatment of the Volkov–Mikhailov model in the QHE regime were pointed out in references [6–8].

Another distinct fully quantum mechanical edge-wave mechanism has been proposed [9–11]. However, for $\nu = 1$, only the edge position of an incompressible 2DEG varies, and the approach is limited to the subspace of wave functions of the lowest LL, neglects level mixing and dissipation and also leads to a single chiral EMP with dispersion similar to that in the Volkov–Mikhailov model.

In this paper, we provide a further step in the theory of EMPs by effectively incorporating the previous two distinct edge-wave mechanisms [3]. In particular, we take into account the LL structure for integer ν, LL mixing and dissipation; it appears that damping of EMPs is fundamentally related to LL mixing. In doing so, we have assumed that the QHE regime holds, the confining potential is sufficiently steep at the edges that the dissipation is significant [12,13]

only within a distance from the edge of the order of the magnetic length $\ell_0 = \sqrt{[\hbar/|e|B]}$ and that LL flattening [14] can be neglected [15, 16]. We show that, for $\nu > 2$, the Coulomb interaction between the charge excitations at the edges of different occupied LLs leads to a repulsion of the uncoupled fundamental LL modes. The new modes, which are nearly undamped, have very different group velocities.

For the 2D system with a vertical conductivity drop at the boundaries, it has been shown [1] that the dissipation significantly affects the dispersion relation and the spatial structure of the EMP even in the regime of the QHE. The properties of the EMP have been expressed in terms of the components of the magnetoconductivity tensor of an infinite 2D system. Moreover, due to the very low frequency ω of the EMP, the dispersion relation can be written in terms of the static magnetoconductivity tensor. However, previous studies [12, 13] by two of the present authors have shown that, for a sufficiently smooth lateral confinement and in the QHE regime, the dissipation appears dominantly due to intra-level–intra-edge transitions of electrons scattered by acoustic phonons and occurs mainly near the edges. For instance, in GaAs-based samples, piezoelectrical phonons are typically involved. In the linear response regime, this is the main cause of dissipation in channels of width $W \lesssim 100$ μm and for temperatures $T \lesssim 1$ K if the group velocity of the edge states v_g is larger than the speed of sound s. Indeed, in the bulk region of channels, the dissipation is exponentially suppressed as the temperature goes to zero. Under these conditions and in view of the fact that the dissipation is homogeneous over the channel width in the Volkov–Mikhailov model [1], the previous results of Balev and Vasilopoulos [3, 17] are understood as a demonstration that the EMP properties reported in reference [1] can be strongly modified by dissipative processes localized near the channel edges. Here we assume very low temperatures such that the condition $k_B T \ll \hbar v_g/\ell_0$ is fulfilled. A brief account of some results of the present investigation has appeared in reference [3]. Here we elaborate on our EMP theory and provide new additional material which can make results more accessible to a broader audience. The notation that is used here coincides with that in reference [3] with two exceptions: (i) here we denote $e^2/\pi\hbar$ as $\tilde{\sigma}^0_{yx}$, reserving the notation σ^0_{yx} for the Hall conductivity in the bulk region (i.e., for $\nu = 2$, $\tilde{\sigma}^0_{yx}$ and σ^0_{yx} coincide, while for $\nu = 4$, they are different); (ii) for the inter-LL length we use the term $\Delta y_{01} = y_{r0} - y_{r1}$, instead of Δy.

The organization of the paper is as follows. In section 2, starting with the expressions for the inhomogeneous current densities and conductivities, we derive the integral equation for the EMP and present the general method for solving it. In section 3 we calculate the dispersion relations and the spatial structure of the new edge waves at very low temperatures. Finally, in section 4 we compare our theory with experiment and present our concluding remarks.

2. Basic relations

2.1. Inhomogeneous current density in the quasi-static regime

We consider a 2DEG confined to a strip in the x–y plane with a width W along the y-axis and length L along a channel in the x-direction, under a strong magnetic field $\boldsymbol{B}$ parallel to the z-axis. For simplicity, we consider the confining potential as parabolic at the edges, such that $V_y = 0$ for $y_l < y < y_r$, $V_y = m^*\Omega^2(y - y_r)^2/2$ for $y > y_r > 0$ and $V_y = m^*\Omega^2(y - y_l)^2/2$ for $y < y_l < 0$, where $y_{r\,(l)}$ delimits the right-hand (left-hand) edge of the flat part of V_y. We also assume that the condition $|k_x|W \gg 1$ is satisfied, so it is possible to consider an EMP along the right-hand edge of the channel of the form $A(\omega, k_x, y)\exp[-\mathrm{i}(\omega t - k_x x)]$ totally independent of the left-hand edge. We restrict consideration to the linear response regime. For definiteness, we take the background dielectric constant ϵ to be spatially homogeneous. In the

QHE regime and with ν even, we neglect the Zeeman spin splitting. As for the case where $\nu = 1$, we assume that the spin splitting, caused by many-body effects, is strong enough that we can discard the contribution related to the upper spin-split LL. We also assume a smooth lateral confinement on the scale of the magnetic length $\ell_0 = (\hbar/m^*\omega_c)^{1/2}$ such that $\Omega \ll \omega_c$, where $\omega_c = |e|B/m^*$ is the cyclotron frequency.

Due to the low-frequency limit for the EMP ($\omega \ll \omega_c$), the current density can be evaluated within a quasi-static approximation by using the fact that the EMP's wavelength λ is much larger than ℓ_0. Following references [3] and [17], we write the components of the current density in the form

$$j_y(y) = \sigma_{yy}(y)E_y(y) + \sigma^0_{yx}(y)E_x(y) \tag{1}$$

$$j_x(y) = \sigma_{xx}(y)E_x(y) - \sigma^0_{yx}(y)E_y(y) + \sum_j v_{gj}\rho_j(\omega, k_x, y) \tag{2}$$

where $\sigma_{\mu\gamma}(y)$ and $E_\gamma(y)$ are the components of the conductivity tensor and the electric field respectively. Here we have suppressed the exponential factor $\exp[-\mathrm{i}(\omega t - k_x x)]$ common to all terms in equations (1) and (2). It is understood that $E_\gamma(y)$ depends on ω and k_x. The term $v_{gj}\rho_j(\omega, k_x, y)$ represents an advection contribution caused by a charge distortion $\rho_j(\omega, k_x, y)$ localized near the edge y_{rj} of the jth LL. In equations (1) and (2) the contributions to $j_\mu(y)$, which are proportional to $E_\gamma(y)$, are obtained microscopically when the electric field is smooth on the scale of ℓ_0. Even though this is not well justified for both components proportional to $E_x(y)$ and $E_y(y)$, we approximate these contributions by those obtained when $E_x(y)$ and $E_y(y)$ are smooth on the scale of ℓ_0. This approximation is equivalent to neglecting nonlocal contributions to j_μ that are $\propto \int \mathrm{d}y'\,\sigma_{\mu\gamma}(y, y')E_\gamma(y')$. For weak dissipation, this can be justified within a treatment based on the random-phase approximation (RPA) [18] that includes nonlocal effects and edge-state screening, e.g., for the fundamental EMPs at $\nu = 2, 4, 6$. The Hall conductivity is [13]

$$\sigma^0_{yx}(y) = \frac{e^2}{2\pi\hbar}\sum_{n=0}\int_{-\infty}^{\infty}\mathrm{d}y_{0\alpha}\; f_\alpha \Psi_n^2(y - y_{0\alpha}) \tag{3}$$

where $\alpha \equiv \{n, k_{x\alpha}\}$, $y_{0\alpha} = \ell_0^2 k_{x\alpha}$, $\Psi_n(y)$ is the harmonic oscillator function and

$$f_\alpha \equiv f_n(k_{x\alpha}) = 1/[1 + \exp(\varepsilon_\alpha - \varepsilon_F)/k_B T]$$

is the Fermi–Dirac function. ε_F is the Fermi level measured from the bottom of the lowest electric subband; for even ν, the right-hand side of equation (3) should be multiplied by 2, the spin degeneracy factor. We point out that, for $\nu = 1$ and $T = 0$ and near the right-hand edge, we obtain

$$\sigma^0_{yx}(y) = (e^2/4\pi\hbar)[1 + \Phi(y_{re} - y)]$$

where $\Phi(x)$ is the probability integral, $y_{re} = \ell_0^2 k_{re}$ and $f_0(k_{re}) = 1/2$. Notice that $\sigma^0_{yx}(y)$, near the edge, decreases on the scale of ℓ_0 and behaves like the density profile depicted by the dashed curve of figure 1. Considering only the right-hand edge and the flat part of the confining potential for $y_l \leqslant y_{0\alpha} \leqslant y_r$, we obtain the energy levels $\varepsilon_\alpha = \hbar\omega_c(n + 1/2)$ and, for $y_{0\alpha} \geqslant y_r$, the energy spectrum can be written as

$$\varepsilon_\alpha \equiv \varepsilon_n(k_{x\alpha}) = \hbar\omega_c(n + 1/2) + m^*\Omega^2(y_{0\alpha} - y_r)^2/2. \tag{4}$$

This result implies that $\varepsilon_{\bar{n}}(k_{x\alpha})$, as a function of $y_{0\alpha}$, is smooth on the scale of $[\sqrt{(2\bar{n} + 1)}]\ell_0$, where $\bar{n}$ is the principal quantum number of the highest occupied LL. The energy spectrum (4) of the nth LL allows us to evaluate the group velocity of the edge states as

$$v_{gn} = \partial\varepsilon_n(k_r + k_e^{(n)})/\hbar\,\partial k_x = \hbar\Omega^2 k_e^{(n)}/m^*\omega_c^2$$

with the characteristic wave vector

$$k_e^{(n)} = (\omega_c/\overline{h}\Omega)\sqrt{2m^*\Delta_{Fn}} \qquad \text{where } \Delta_{Fn} = \varepsilon_F - (n+1/2)\overline{h}\omega_c.$$

The edge of the nth LL is denoted by $y_{rn} = y_r + \ell_0^2 k_e^{(n)} = \ell_0^2 k_{rn}$, where $k_{rn} = k_r + k_e^{(n)}$, $k_r = y_r/\ell_0^2$ and $W = 2y_{r0}$. We can also write $v_{gn} = E_{en}/B$, where $E_{en} = \Omega\sqrt{2m^*\Delta_{Fn}}/|e|$ is the electric field associated with the confining potential V_y at y_{rn}.

We consider only the electron–phonon interaction and neglect that of electrons with impurities, since the former is the most essential for the assumed conditions [12]. Following references [17] and [3], we approximate $\sigma_{xx}(y)$ by

$$\sigma_{yy}(y) = \sum_{n=0}^{\bar{n}} \sigma_{yy}^{(n)}(y).$$

Furthermore, at very low T, where $\overline{h}v_{gn} \gg \ell_0 k_B T$ with $v_{gn} > s$ satisfied, equation (16) of reference [13] gives $\sigma_{yy}^{(n)}(y) = \tilde{\sigma}_{yy}^{(n)}\Psi_n^2(\bar{y}_n)$, where $\bar{y}_n = y - y_{rn}$. For piezoelectrical phonons and $\nu = 2, 4$, we have

$$\tilde{\sigma}_{yy}^{(n)} = 3e^2\ell_0^4 c' k_B^3 T^3/\pi^2\overline{h}^6 v_{gn}^4 s$$

where c' is the electron–phonon coupling constant. For piezoelectrical phonons in a GaAs-based heterostructure, $c' = \overline{h}(eh_{14})^2/(2\rho_V s)$, where $h_{14} = 1.2 \times 10^9$ V m^{-1}, $\rho_V = 5.31 \times 10^3$ kg m^{-3}, $s = 2.5 \times 10^3$ m s^{-1}. Note that $\sigma_{yy}(y)$ is exponentially localized within a distance $\lesssim \ell_0$ from the LL edge y_{rn}. Notice also that for $v_{gn}/s \gg 1$ such that $s/\sqrt{2}v_{gn} < k_B T\ell_0/\overline{h}v_{gn} \ll 1$, we have

$$\tilde{\sigma}_{yy}^{(n)} = \sqrt{2}e^2\ell_0^3 c' k_B^2 T^2/\pi^{5/2}\overline{h}^5 v_{gn}^4.$$

Furthermore, for all cases it is assumed that the strong-magnetic-field condition, namely $\sigma_{yy}(y)/|\sigma_{yx}^0(y)| \ll 1$, is fulfilled.

2.2. The integral equation for EMPs with dissipation at the edges

Using equations (1)–(3), the Poisson equation and the linearized continuity equation, we obtain the following integral equation for $\rho(\omega, k_x, y)$:

$$-\mathrm{i}\sum_n(\omega - k_x v_{gn})\rho_n(\omega, k_x, y) + \frac{2}{\epsilon}\Bigg[k_x^2\sigma_{xx}(y) - \mathrm{i}k_x\frac{\mathrm{d}}{\mathrm{d}y}[\sigma_{yx}^0(y)] - \sigma_{yy}(y)\frac{\mathrm{d}^2}{\mathrm{d}y^2} - \frac{\mathrm{d}}{\mathrm{d}y}[\sigma_{yy}(y)]\frac{\mathrm{d}}{\mathrm{d}y}\Bigg] \times \int_{-\infty}^{\infty}\mathrm{d}y'\, K_0(|k_x||y - y'|)\rho(\omega, k_x, y') = 0 \tag{5}$$

where $K_0(x)$ is the modified Bessel function. For the dissipationless classical 2DEG, equation (5) becomes identical with equation (4) of reference [2]. Furthermore, if the conductivity components are independent of y, for $|y| < W/2$ equation (5) assumes the form of equation (15) of reference [1]. In order to solve equation (5), we note that, for $\overline{h}v_{gn} \gg \ell_0 k_B T$, we have

$$\mathrm{d}[\sigma_{yx}^0(y)]/\mathrm{d}y \propto \sum_{n=0}^{\bar{n}}\Psi_n^2(\bar{y}_n)$$

whose spatial behaviour is similar to that of $\sigma_{yy}(y)$. Then equation (5) shows that $\rho_n(\omega, k_x, y)$ will be concentrated within a region of extent of the order of ℓ_0 around the edge of the nth LL. Furthermore, the integral can be evaluated under the assumption that $k_x\ell_0 \ll 1$ and using

the approximation $K_0(|x|) \approx \ln(2/|x|) - \gamma$, where γ is the Euler constant. Assuming that $\Delta y_{m-1,m} = y_{rm-1} - y_{rm} \gg \ell_0$ (see figure 1 for $\nu = 4$), we can neglect the exponentially small overlap between $\rho_{m-1}(\omega, k_x, y)$ and $\rho_m(\omega, k_x, y)$ for $m \leqslant \bar{n}$. It is then natural to attempt to find an exact solution of the form

$$\rho(\omega, k_x, y) = \sum_{n=0}^{\bar{n}} \rho_n(\omega, k_x, y) = \sum_{n=0}^{\bar{n}} \Psi_n^2(\bar{y}_n) \sum_{l=0}^{\infty} \rho_n^{(l)}(\omega, k_x) H_l(\bar{y}_n/\ell_0) \tag{6}$$

where we have used the Hermite polynomials $H_l(x)$ as the expansion basis. We call the terms with $l = 0$, $l = 1$, $l = 2$ (and so on), the monopole, dipole, quadrupole terms in the expansion of $\rho_n(\omega, k_x, y)$ relative to $y = y_{rn}$.

2.3. EMPs for $\nu = 2$ and $\nu = 4$

Below we first present the general formulae for the case where $\nu = 4$ ($\bar{n} = 1$). Using them, we show how the general formulae for $\nu = 2$ ($\bar{n} = 0$) follow. For $\nu = 4$ we multiply equation (5) by $H_m(\bar{y}_0/\ell_0)$ and integrate over y, from $y_{r0} - \Delta y_{01}/2$ to $y_{r0} + \Delta y_{01}/2$. Analogous integration, from $y_{r1} - \Delta y_{01}/2$ to $y_{r1} + \Delta y_{01}/2$, is repeated with $H_{m_1}(\bar{y}_1/\ell_0)$. With the abbreviations $\rho_0^{(m)}(\omega, k_x) \equiv \rho_0^{(m)}$, $a_{mk}(k_x) \equiv a_{mk}$ etc, we obtain the following coupled systems of equations:

$$(\omega - k_x v_{g0})\rho_0^{(m)} - (S_0 + mS_0') \sum_{n=0}^{\infty} c_{mn} a_{mn} \rho_0^{(n)} - (S_0 + mS_0') \sum_{l=0}^{\infty} c_{ml} b_{ml} \rho_1^{(l)} = 0 \tag{7}$$

$$\begin{aligned}(\omega - k_x v_{g1})&\left[A_{m_1}\rho_1^{(m_1)} + B_{m_1}\rho_1^{(m_1+2)} + \rho_1^{(m_1-2)}/2\right] \\ &- (S_1 + m_1 S_1')\left[\sum_{n=0}^{\infty} c_{m_1 n}\, b_{n m_1} \rho_0^{(n)} + \sum_{j=0}^{\infty} c_{m_1 j} d_{m_1 j} \rho_1^{(j)}\right] \\ &+ 2\sqrt{m_1} S_1' \left[\sum_{n=0}^{\infty} c_{m_1 n}\, \tilde{b}_{n,m_1} \rho_0^{(n)} + \sum_{j=0}^{\infty} c_{m_1 j} \tilde{d}_{m_1,j} \rho_1^{(j)}\right] = 0\end{aligned} \tag{8}$$

where

$$a_{mn} = a_{nm} = \int_{-\infty}^{\infty} \mathrm{d}x\ \Psi_m(x)\Psi_0(x) \int_{-\infty}^{\infty} \mathrm{d}x'\ K_0(|k_x||x - x'|)\Psi_n(x')\Psi_0(x') \tag{9}$$

and

$$b_{mn} = \int_{-\infty}^{\infty} \mathrm{d}x\ \Psi_m(x)\Psi_0(x) \int_{-\infty}^{\infty} \mathrm{d}x'\ 2(x'/\ell_0)^2 K_0(|k_x||x - x' + \Delta y_{01}|)\Psi_n(x')\Psi_0(x'). \tag{10}$$

The other coefficients are given as

$$\tilde{b}_{mn} = \int_{-\infty}^{\infty} \mathrm{d}x\ \Psi_m(x)\Psi_0(x) \int_{-\infty}^{\infty} \mathrm{d}x'\ K_0(|k_x||x - x' + \Delta y_{01}|)\Psi_{n-1}(x')\Psi_1(x') \tag{11}$$

$$d_{mn} = (2/\ell_0^2) \int_{-\infty}^{\infty} \mathrm{d}x\ \Psi_m(x) x \Psi_1(x) \int_{-\infty}^{\infty} \mathrm{d}x'\ K_0(|k_x||x - x'|)\Psi_n(x')x'\Psi_1(x') \tag{12}$$

and

$$\tilde{d}_{mn} = (\sqrt{2}/\ell_0) \int_{-\infty}^{\infty} \mathrm{d}x\ \Psi_{m-1}(x)\Psi_1(x) \int_{-\infty}^{\infty} \mathrm{d}x'\ K_0(|k_x||x - x'|)\ \Psi_n(x')x'\Psi_1(x'). \tag{13}$$

In addition,

$$\begin{aligned} &c_{mn} = \sqrt{2^n n!/2^m m!} \\ &A_{m_1} = (2m_1 + 1) \qquad\qquad B_{m_1} = (m_1 + 2)(2m_1 + 2) \\ &S_j = 2(k_x \tilde{\sigma}_{yx}^0 - \mathrm{i}k_x^2 \tilde{\sigma}_{xx}^{(j)})/\epsilon \qquad S_j' = -4\mathrm{i}\tilde{\sigma}_{yy}^{(j)}/\epsilon\ell_0^2 \end{aligned}$$

and $\tilde{\sigma}^0_{yx} = e^2/\pi\overline{h}$. Notice that here in the interior part of the channel $\sigma^0_{yx}(y) = \sigma^0_{yx} = 2\tilde{\sigma}^0_{yx} = 2e^2/\pi\overline{h}$.

Furthermore, for $\nu = 2$ ($\bar{n} = 0$), the third term in equations (7) and (8) is absent and we obtain explicitly

$$(\omega - k_x v_{g0})\rho_0^{(m)} - (S_0 + mS_0')\sum_{n=0}^{\infty} c_{mn}a_{mn}\rho_0^{(n)} = 0. \tag{14}$$

In this case we obtain that $\sigma^0_{yx}(y) = \sigma^0_{yx} = \tilde{\sigma}^0_{yx} = e^2/\pi\overline{h}$ for the inner part of the channel.

3. Edge waves

3.1. Edge modes for $\nu = 2$ (1)

In what follows we assume that $\nu = 2$, but the results obtained can easily be extended to the case where $\nu = 1$, when only the lowest spin-split LL is occupied. Equations (6) and (14) show that there exist independent modes which are spatially *symmetric*, $\rho^s(\omega, k_x, y)$, or *antisymmetric*, $\rho^a(\omega, k_x, y)$, with respect to $y = y_{r0}$ (see reference [17]). They correspond in equation (6) to l even and odd respectively. Notice that in this case $\bar{n} = 0$, and all edge modes belong to the $n = 0$ LL. However, within our quasi-microscopic approach, the mixing of the $n = 0$ LL with some higher empty LLs is included.

We first consider the lowest antisymmetric mode for *weak dissipation* [17] $\eta = \tilde{\sigma}^{(0)}_{yy}/(\ell_0^2\sigma^0_{yx}|k_x|) \ll 1/4$. On neglecting its coupling with higher antisymmetric modes, it becomes purely dipolar and corresponds to $l = 1$ and $n = 0$ in equation (6). To take into account the effect of inter-mode coupling on this pure dipole mode, we will neglect the damping. Then, as shown in reference [17], the pure dipole mode has a dimensionless velocity $v_{dip} = (\omega/k_x - v_{g0})/(2\sigma^0_{yx}/\epsilon)$ which gives $v_{dip} = a_{11} \approx 0.4996$. Furthermore, if the interaction of this mode with the octupole mode ($l = 1$) is considered (i.e. only the $l = 1$ and $l = 3$ terms in equation (6) are retained), the velocity of the renormalized dipole mode becomes

$$v_{dip} = (a_{11} + a_{33} + \sqrt{(a_{11} - a_{33})^2 + 4a_{13}^2})/2 \approx 0.5963.$$

So, due to the interaction with the $l = 3$ mode, v_{dip} becomes ≈20% higher. To consider further the interaction of the dipole mode with the $l = 3$ and $l = 5$ modes, we retain the terms $l = 1, 3$ and $l = 5$ in equation (6). From equation (14), for $m = 1, 3$ and $m = 5$, we obtain a system of three linear equations for $\rho_0^{(1)}$, $\rho_0^{(3)}$ and $\rho_0^{(5)}$ that leads to $v_{dip} \approx 0.6287$, which is only almost 5% higher than that when only the terms with $l = 1, 3$ were retained. Apparently v_{dip}, and consequently the dispersion relation of the dipole mode, exhibits fast convergence when higher-order l-terms are taken into account in the series expansion. Notice that, within the present approach, the dipole mode has a purely acoustic dispersion. The charge-density profile $\delta\rho(y)$ of the dipole mode is depicted in figure 2, where we plot

$$\delta\rho(y) \equiv \tilde{\rho}(v_{dip}, y) = \sqrt{\pi}\ell_0\rho(\omega_{dip}(k_x), k_x, y)/\rho^{(1)}(\omega_{dip}(k_x), k_x)$$

as a function of $\bar{y}_0/\ell_0$. The dashed, short-dashed and solid curves are obtained, respectively, with one ($l = 1$), two ($l = 1, 3$) or three ($l = 1, 3, 5$) terms retained in expansion (6). The profile already exhibits a clear convergence for $l \leqslant 5$.

For *very strong dissipation* $\eta \gg K$, where $K = \ln(1/|k_x\ell_0|) + 1/2$, all of the branches are strongly damped except the one EMP mode, so we discuss here the latter EMP branch which is weakly damped and was termed the *low-frequency edge helicon* (LFEH) in references [17] and [3]. This mode is spatially symmetric and its real part

$$\mathrm{Re}\,\omega(k_x) \equiv \mathrm{Re}\,\omega_{EH}^{LF} \approx k_x v_{g0} + (2\sigma^0_{yx}k_x/\epsilon)(K - 1/4)$$

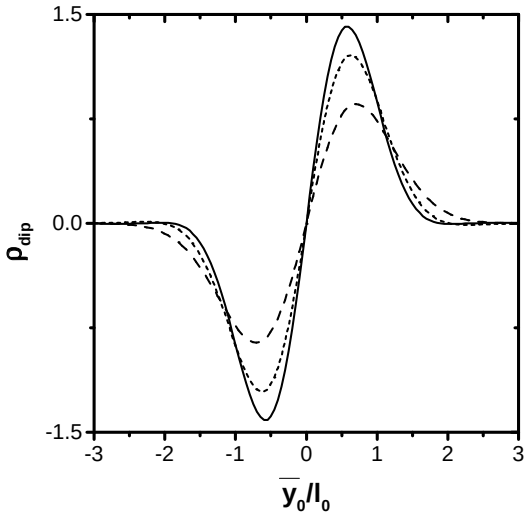

Figure 2. Dimensionless charge-density profiles $\widetilde{\rho}(y) \equiv \rho_{dip}$ for the dipole mode as functions of $\bar{y}_0/\ell_0$; $\nu = 1, 2$ and $\overline{n} = 0$. The dashed, short-dashed and solid curves correspond to one ($l = 1$), two ($l = 1, 2$) and three ($l = 1, 2, 3$) terms, respectively, retained in the expansion (equation 6).

is very close to Re $\omega(k_x)$ for the fundamental EMP of the $n = 0$ LL, namely,

$$\mathrm{Re}\,\omega_{EH}^{(0)} \approx k_x v_{g0} + (2\sigma_{yx}^0 k_x/\epsilon)(K + 1/4).$$

It is convenient now to point out the results of references [3] and [17] concerning the properties of the fundamental EMP of the $n = 0$ LL. Its dispersion is given by

$$\omega_{EH}^{(0)} = k_x v_{g0} + S_0\ (K + 1/4) + S_0'/4K$$

for both *weak dissipation* ($\eta \ll 1/4$) and *strong dissipation* ($K \gg \eta \gg 1/4$). In the latter case, the fundamental EMP was termed the *high-frequency edge helicon* (HFEH). In both regimes of dissipation, this EMP has mainly monopole character: in the first case, its density profile satisfies the condition $|\rho_0^{(2)}/\rho_0^{(0)}| \approx (1/8K) \ll 1$; and in the second case, $|\rho_0^{(2)}/\rho_0^{(0)}| \approx (\eta/2K) \ll 1$. In either regime, considering only two terms in equation (6), those with $l = 0$ and $l = 2$, is well justified. This is not the case for the LFEH as shown in reference [3].

To support the statements made above, we present in figures 3 and 4 the evolution of the real and imaginary parts of the dimensionless charge density for the LFEH given by

$$\delta\rho_r = \sqrt{\pi}\ell_0\ \mathrm{Re}[\rho(\omega, k_x, y)/\rho_0^{(0)}(\omega, k_x)]$$

and

$$\delta\rho_i = \sqrt{\pi}\ell_0\ \mathrm{Im}[\rho(\omega, k_x, y)/\rho_0^{(0)}(\omega, k_x)]$$

respectively, as one increases the number of terms considered in the expansion for $K/\eta = 0.01$. Notice that, while $\delta\rho_r$ represents the charge profile for a particular phase of the wave, $\delta\rho_i$ represents it for the phase shifted by $\pm\pi/2$. Since $\delta\rho(y)$ is symmetric with respect to the edge, only half of the profile is shown in figures 3 and 4. In figure 3, curve 1 represents $\delta\rho_r$ when only the $l = 0$ term is retained in the expansion and curve 2 shows

$$\delta\rho_r \approx \sqrt{\pi}\ell_0[\Psi_0^2(\bar{y}_0) + \sqrt{2}\Psi_2(\bar{y}_0)\Psi_0(\bar{y}_0)]$$

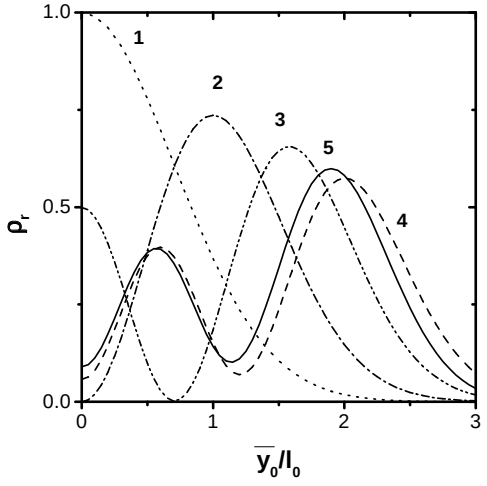

Figure 3. The dimensionless charge-density profile $\rho_r \equiv \mathrm{Re}\,\delta\rho$ of the low-frequency edge helicon (LFEH) as a function of $\bar{y}_0/\ell_0$ for $K/\eta = 0.01$; $\nu = 1, 2$ and $\overline{n} = 0$. The numbers of *even* terms retained in equation (6) are shown next to the curves.

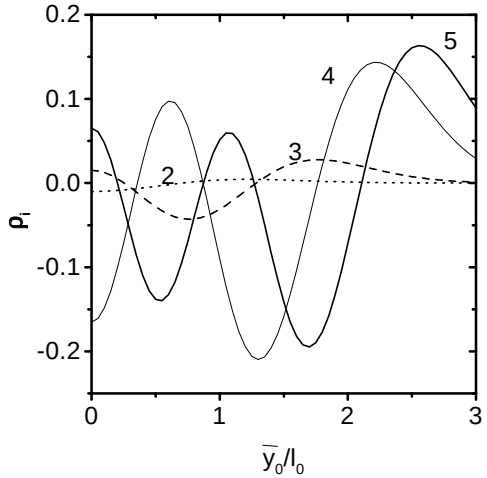

Figure 4. The dimensionless charge-density profile $\rho_i \equiv \mathrm{Im}\,\delta\rho$ of the low-frequency edge helicon (LFEH) as a function of $\bar{y}_0/\ell_0$ for $K/\eta = 0.01$; $\nu = 1, 2$ and $\overline{n} = 0$. The numbers of *even* terms retained in equation (6) are shown next to the curves.

when two terms ($l = 0, 2$) are retained. Because these curves are fundamentally different, more l-terms should be considered in equation (6). Thus, to describe better the profile $\delta\rho_r$, we also plot curves 3, 4 and 5 obtained, respectively, when three, four and five even-l terms are retained in equation (6), corresponding to the solution of systems of three, four and five equations following from equation (14). For instance, curve 5 was obtained by retaining the terms with $l = 0, 2, 4, 6$ and 8 along with equations for $m = 0, 2, 4, 6$ and 8. As is seen in figure 3, retaining four or five terms in the l-summation already leads to a rapid convergence in $\delta\rho_r$ without much change in either the oscillatory character or the magnitude. In figure 4, similar results are depicted for the profile $\delta\rho_i$ when two, three, four and five even-l terms are retained in equation (6). Notice that the contribution due to the monopole term, with $l = 0$, is absent because the total edge charge $\int \mathrm{d}y\ \delta\rho_i = 0$. Therefore $\delta\rho_i$ must show a substantially stronger oscillatory behaviour than $\delta\rho_r$ and correspondingly a slower convergence, in agreement with figures 3 and 4. However, curves 4 and 5 in figure 4 have approximately the same magnitude in the region where $|\bar{y}_0|/\ell_0 \leqslant 1.5$. Moreover, for $|\bar{y}_0|/\ell_0 \geqslant 1.5$ these curves exhibit the same spatial behaviour and magnitude. This means that the expansion for $\delta\rho_i$ already essentially demonstrates convergence with four and five terms taken into account; however, in these cases, due to the absence of a contribution from the lowest ($l = 0$) term in this expansion, only three and four l-terms in effect contribute to the spatial structure—namely those with $l = 2, 4, 6$ and those with $l = 2, 4, 6, 8$, respectively.

In figures 5 and 6, we plot the same profiles as in figures 3 and 4, respectively, for $K/\eta = 0.1$. Curves 1 and 2 in figure 5 show $\delta\rho_r$ with, respectively, only one ($l = 0$) or two ($l = 0, 2$) terms retained in equation (6). As can be seen, retaining three, four or five terms in the l-summation already leads to a clear convergence of the form of $\delta\rho_r$. Figure 6 shows the profile $\delta\rho_i$ and the curves are labelled as in figure 4. Because the contribution of the monopole term is absent, $\delta\rho_i$ has an essentially oscillatory behaviour that is rather similar for curves 4 and 5, as the spatial positions of the extrema for the two curves almost coincide. This means that despite substantially slower convergence of the expansion for $\delta\rho_i$, due to the absence of

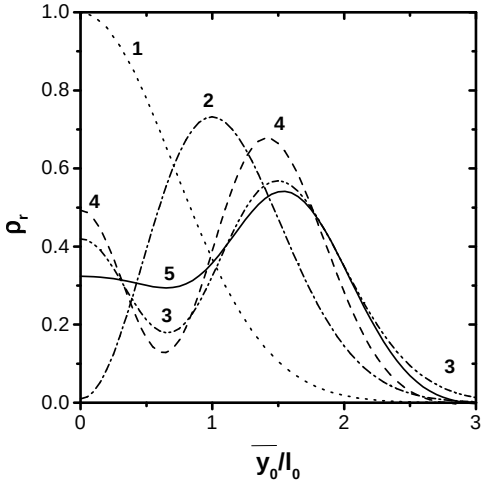

Figure 5. As figure 3, but for $K/\eta = 0.1$.

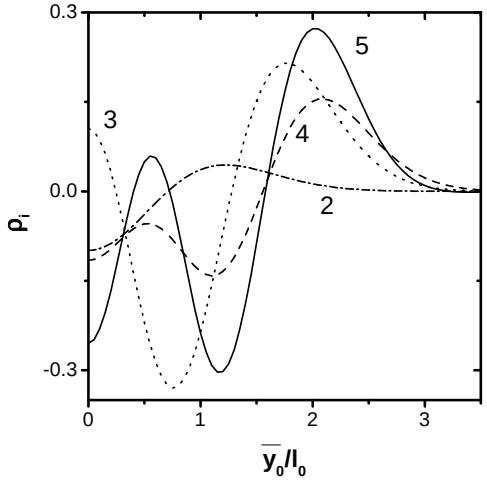

Figure 6. As figure 4, but for $K/\eta = 0.1$.

the lowest ($l = 0$) term (which in turn leads to strongly oscillatory behaviour of $\delta\rho_i$ along y, in contrast to that of $\delta\rho_r$), curves 4 and 5 in figure 6 already essentially demonstrate convergence. However, in contrast to the case for $\delta\rho_r$, for these two curves, due to the trivial contribution from the $l = 0$ term to $\delta\rho_i$, in effect only three ($l = 2, 4, 6$) and four ($l = 2, 4, 6, 8$) l-terms contribute.

The dispersion relation of the LFEH obtained for the cases represented by curves 2 in figures 3–6 is given by [3, 17]

$$\omega_{EH}^{LF} = k_x v_{g0} + \{(2\sigma_{yx}^0 k_x/\epsilon) - [\mathrm{i}\tilde{\sigma}_{yy}^{(0)}/\eta^2\ell_0^2\epsilon]\}(K - 1/4). \tag{15}$$

When more l-terms are taken into account, only the imaginary part Im ω_{EH}^{LF} changes significantly. For instance, with two, three, four or five terms retained and $K/\eta = 0.01$, the dispersion relations, corresponding to figures 3 and 4, are given, respectively, by

$$\Omega_{EH}^{LF} = \omega_{EH}^{LF}/S_0 \approx [(K - 0.25) - 0.005\mathrm{i}] \qquad \Omega_{EH}^{LF} \approx [(K - 0.50) - 0.062\mathrm{i}]$$
$$\Omega_{EH}^{LF} \approx [(K - 0.63) - 0.117\mathrm{i}] \qquad \Omega_{EH}^{LF} \approx [(K - 0.57) - 0.133\mathrm{i}].$$

It is clearly seen that on taking into account four and five even terms, Im ω_{EH}^{LF} shows rapid convergence to its exact value. Despite the *very strong dissipation*, the LFEH is *very weakly damped* since $\mathrm{Re}|\omega_{EH}^{LF}| \gg \mathrm{Im}|\omega_{EH}^{LF}|$. Furthermore, in contrast with the case for reference [1], Re ω_{EH}^{LF} is independent of T and the damping rate Im ω_{EH}^{LF} is not quantized but varies as T^{-3} or T^{-2}; the latter holds if $s/\sqrt{2}v_{g0} < k_B T\ell_0/\hbar v_{g0} \ll 1$. We point out that if, e.g., five l-terms are taken into account, then all of them contribute to ω_{EH}^{LF} and $\delta\rho_r$; however, only four l-terms will effectively contribute to $\delta\rho_i$.

Due to specific properties of the LFEH, such as the essential charge oscillations transverse to the edge, we may distinguish the LFEH from the fundamental EMP of the $n = 0$ LL. For *strong dissipation* the latter mode is also called the HFEH of the $n = 0$ LL. It is worth noticing that for the fundamental mode we have $2(Kk_x\ell_0)^2 \ll 1$ due to the long-wavelength condition $k_x\ell_0 \ll 1$. Therefore S_j can be approximated well by its real part for the fundamental mode.

3.2. The repulsion of fundamental EMPs for $\nu = 4$

Although here the condition $\Delta y_{01}/\ell_0 \gg 1$ is well justified, as can be seen in figure 1, and simplifies the treatment, the system of equations (7) and (8) can be strongly coupled by the long-range Coulomb interaction between the edges of the LLs. However, if this inter-edge Coulomb coupling is neglected in equations (7) and (8), on setting the coefficients b_{mn} and $\tilde{b}_{mn}$ equal to zero, equation (7) leads to equation (14) for the $\nu = 2$ case and all edge modes of the $n = 1$ LL are decoupled from those of the $n = 0$ LL.

Now, by taking the decoupling limit, we first consider the symmetric edge modes of the $n = 1$ LL and the cases of *strong* and *weak dissipation*. In the former case, the fundamental mode of the $n = 1$ LL can be called the HFEH of the $n = 1$ LL. To treat the fundamental mode of the $n = 1$ LL properly it is sufficient to consider just the first two even terms in the sum over l in equation (6), namely $\rho_1^{(0)}$ and $\rho_1^{(2)}$: here we must retain only the terms with $n = 1$. Then, from equation (8) for $m_1 = 0$ and $m_1 = 2$, we obtain a system of two linear equations for $\rho_1^{(0)}$, $\rho_1^{(2)}$. The corresponding dispersion relation of the HFEH of the $n = 1$ LL becomes

$$\omega_{EH}^{(1)} \approx k_x v_{g1} + S_1(K - 1/4) + S_1'/12K.$$

The other branch has the dispersion

$$\omega_3^{(1)} \approx k_x v_{g1} + (S_1 + 2S_1')/4.$$

In analogy with the fundamental EMP of the $n = 0$ LL, the $n = 1$ LL fundamental EMP, decoupled from the excitations of the $n = 0$ LL, is very weakly damped even for *strong dissipation*. Now if we omit the term in $\rho_1^{(2)}$ in equation (6), i.e., on neglecting the interaction between the monopole and quadrupole excitations of the $n = 1$ LL, the decoupled fundamental mode of the $n = 1$ LL has a dispersion relation given by $\omega_{EH}^{(1)}$ without the damping term. This holds for the $n = 0$ LL as well, i.e., for its purely monopole excitation $\rho_0^{(0)}$, the dispersion is given by $\omega_{EH}^{(0)}$ without the damping term.

If we take into account the Coulomb coupling between the pure monopole modes $\rho_0^{(0)}$ and $\rho_1^{(0)}$, their dispersions change drastically. For $|k_x|\,\Delta y_{01} \ll 1$, the dispersion of the renormalized fundamental mode of the $n = 0$ LL becomes

$$\omega_+^{(01)} \approx k_x(v_{g0} + v_{g1})/2 + (2/\epsilon)k_x\tilde{\sigma}_{yx}^0[2\ln(1/k_x\ell_0) - \ln(\Delta y_{01}/\ell_0) + 3/5]$$

and that of the $n = 1$ LL becomes

$$\omega_-^{(01)} \approx k_x(v_{g0} + v_{g1})/2 + (2/\epsilon)k_x\tilde{\sigma}_{yx}^0[\ln(\Delta y_{01}/\ell_0) + 2/5].$$

The dispersion relation $\omega_+^{(01)}(k_x)$ is similar to that of the fundamental $j = 0$ mode of reference [2] and to the EMP of reference [1], since each of them has a term $\propto k_x \ln(1/k_x)$. Notice that $\omega_+^{(01)}(k_x)$ is essentially different from the frequency of the *decoupled* $n = 0$ LL fundamental mode

$$\omega \approx k_x v_{g0} + (2/\epsilon)\tilde{\sigma}_{yx}^0 k_x[\ln(1/k_x\ell_0) + 3/4].$$

In contrast with $\omega_+^{(01)}(k_x)$, the dispersion of the renormalized fundamental EMP of the $n = 1$ LL, $\omega_-^{(01)}(k_x)$, becomes purely acoustic. Its phase velocity is larger than that of the $j = 1$ mode of reference [2] for $\Delta y_{01}/\ell_0 \geqslant 5$. Here we observe that the term related to the edge velocities, $k_x(v_{g0} + v_{g1})/2$, is typically much smaller than the second term related to the electron–electron interaction. The spatial dependence of $\rho(\omega, k_x, y)$ for the renormalized fundamental mode of the $n = 0$ LL is approximately $\propto[\Psi_0^2(\bar{y}_0) + \Psi_1^2(\bar{y}_1)]$ and that for the renormalized fundamental mode of the $n = 1$ LL is approximately $\propto[\Psi_0^2(\bar{y}_0) - \Psi_1^2(\bar{y}_1)]$.

The above results for $\mathrm{Re}\,\omega(k_x)$ for the coupled fundamental EMPs of the $n = 0$ and $n = 1$ LLs remain practically unchanged if more terms $\rho_0^{(j)}$ and $\rho_1^{(j)}$, for $j \geqslant 1$, are retained. Notice

that, due to the presence of the inter-edge Coulomb interaction, the symmetry of the problem with respect to y_{r0} or y_{r1} is absent and hence, in principle, $\rho_0^{(j)}$ and $\rho_1^{(j)}$, with j even and odd, must be included. Furthermore, taking into account such additional terms leads to essential contributions to the damping rates of the renormalized fundamental EMPs of the $n = 0$ and $n = 1$ LLs. From $\Delta y_{01}/\ell_0 \gg 1$, $k_x\,\Delta y_{01} \ll 1$ and the properties of the coefficients a_{mn}, b_{mn} etc we find that the most important terms in the summations of equation (6) are $\rho_0^{(0)}$, $\rho_0^{(2)}$, $\rho_1^{(0)}$ and $\rho_1^{(2)}$. Calculations show that the *odd* terms here are negligibly small, so they are discarded. Dropping the less important term $\rho_0^{(2)}$, this leads to a system of three coupled equations giving three branches, $\tilde{\omega}_{\pm}^{(01)}$ and $\omega_3^{(01)}$. The dispersion relation of the renormalized fundamental EMP of the $n = 0$ LL is given by

$$\tilde{\omega}_{+}^{(01)} = k_x(v_{g0} + v_{g1})/2 + (2/\epsilon)k_x\tilde{\sigma}_{yx}^{0}[2\ln(1/k_x\ell_0) - \ln(\Delta y_{01}/\ell_0) + 3/5] + S_1'/16K \tag{16}$$

and that of the $n = 1$ LL is

$$\tilde{\omega}_{-}^{(01)} = k_x(v_{g0} + v_{g1})/2 + (2/\epsilon)k_x\tilde{\sigma}_{yx}^{0}[\ln(\Delta y_{01}/\ell_0) + 2/5] + S_1'/\{24[\ln(\Delta y_{01}/\ell_0) + \gamma + 1/4]\}. \tag{17}$$

The coupled fundamental EMPs $\omega_{\pm}^{(01)}$ are very weakly damped. Notice that the neglect of the $\rho_0^{(2)}$-term in the calculation of the damping rates is justified for dissipation at the edge of the $n = 1$ LL substantially greater than that at the edge of the $n = 0$ LL. Indeed, $S_j' \propto v_{gj}^{-4}$ and the group velocity v_{g0} is typically substantially larger than v_{g1}. So, neglecting the inter-edge Coulomb coupling, the damping rate of the $\omega_{EH}^{(1)}$-branch is three times larger than that of the $\omega_{EH}^{(0)}$-branch for $v_{g0}/v_{g1} = \sqrt{3}$.

4. Discussion and concluding remarks

We have introduced a realistic model for the confining edge potential V_y and made it sufficiently steep at the edge that LL flattening [14] can be discarded [15, 16]. Using this model, we develop a quasi-microscopic approach for evaluating the structure and spectrum of the edge magnetoplasma excitations.

We now compare our results, presented in section 3.1, with the experimental ones obtained by Ashoori *et al* [8]. for $\nu = 1$, $T = 0.3$ K and $B = 5.1$ T. Using the experimental value [19] $\Omega = 7.8 \times 10^{11}$ s^{-1}, we obtain $v_{g0} = 8.8 \times 10^3$ m s^{-1}. This leads to $\tilde{\sigma}_{yy}^{(0)} \propto T^3$. By using a typical excited wave vector $q \simeq \pi/2L_p$, where $L_p = 10\ \mu$m is the side of the square pulser (which generates charge pulses), we find that all calculated modes for $\nu = 1$ are quite strongly damped except the fundamental mode $\omega_{EH}^{(0)}$ which is very weakly damped. Its damping rate is $\mathrm{Im}\,\omega_{EH}^{(0)} \approx 2 \times 10^7$ s^{-1} and its period of travel $T_{tr} \approx 3.4$ ns, in agreement with the experimental values.

The EMP dispersion, given by equations (16) and (17), for $\nu = 4$, was compared in figure 3 of reference [3] with the experimental data of reference [4]. Using the same value of Ω as before, one has $\Omega/\omega_c \approx 0.14$, $\Delta y_{01}/\ell_0 \approx 6$, $v_{g0} = 2.3 \times 10^3$ m s^{-1} and $v_{g0}/v_{g1} = \sqrt{3}$. The spectrum of the $\nu = 4$ modes, shown in figure 3(a) of reference [4], is very well described by the dispersion of the renormalized fundamental modes given by equations (16) and (17). The same holds for the $\nu = 4$ mode of figure 3(b) of reference [4]. The mode $\omega_3^{(01)}$ is strongly damped. Taking $\epsilon = 6.75$, its decay rate is

$$\mathrm{Im}\ S_1'/2 \approx 2\tilde{\sigma}_{yy}^{(1)}/\epsilon\ell_0^2 \approx 1.3 \times 10^{10}\ \mathrm{s}^{-1}.$$

The latter is still smaller than that of the $j = 1$ branch of the Aleiner–Glazman model [2], $1/\tau_1 \approx 2 \times 10^{10}$ s^{-1}, which becomes four times larger for $B = 1$ T, due to the B^{-2}-behaviour.

The decay rate of the $j = 0$ mode in this model [2] is $1/\tau_0 \approx 1.7 \times 10^9\ \mathrm{s}^{-1}$ whereas our result for the $\tilde{\omega}_+^{(01)}$-mode, given by equation (16), is about ten times smaller:

$$\mathrm{Im}\ \tilde{\omega}_+^{(01)} \approx 2.1 \times 10^8\ \mathrm{s}^{-1}.$$

Moreover, the damping rate of the $\tilde{\omega}_-^{(01)}$-mode, given by equation (17), is much less than that of the $j = 1$ mode of the Aleiner–Glazman model [2], since we have

$$\mathrm{Im}\ \tilde{\omega}_-^{(01)} \approx 5.6 \times 10^8\ \mathrm{s}^{-1} \ll 1/\tau_1 \approx 2 \times 10^{10}\ \mathrm{s}^{-1}.$$

Thus, the decay rates of the $\tilde{\omega}_\pm^{(01)}$-modes should be much closer to those of the experiment [4] than the previous strongly overestimated results of Aleiner and Glazman [2]. With regard to the delay times t_d, which are directly related to the mode group velocity, for the sample with length $L_x = 320\ \mu$m, we obtain $t_d = 0.12$ ns for the $\tilde{\omega}_+^{(01)}$-mode and $t_d = 0.69$ ns for the $\tilde{\omega}_-^{(01)}$-mode, which is also in excellent agreement with the experimental data, as we can see from figure 3(a) of reference [4]. We can conclude that our results for the renormalized fundamental modes are in quite good agreement with the experimental ones as regards both the spectrum properties (phase and group velocities) and the damping rates. We also stress the conclusion, from the previous discussion, that the slower mode observed [4] for $\nu = 4$ cannot be identified with the $j = 1$ mode of the Aleiner–Glazman model but can be identified with the present $\tilde{\omega}_-^{(01)}$-mode, i.e., the renormalized fundamental EMP of the $n = 1$ LL. In addition, it is also clear that our theory, in contrast with that of reference [2], accounts for the existence of the plateaus [4] in t_d since the quantized Hall conductivity appears spontaneously in all dispersion relations and, moreover, the assumption of the QHE regime is essential to our study.

The properties of the edge waves in the three regimes of *weak* ($\eta \ll 1/4$), *strong* ($1/4 \ll \eta \ll K$) and *very strong* ($\eta \gg K$) dissipation can be summarized as follows. For $\nu = 2$ (1):

(a) The fundamental EMP for the $n = 0$ LL has mainly a monopole character with characteristic dispersion $\omega \propto k_x \ln(1/k_x\ell_0)$ and a weak damping in the regimes of weak and strong dissipation (the high-frequency edge helicon).
(b) For very strong dissipation, one obtains strongly damped branches and only one weakly damped one (the low-frequency edge helicon). The real part of the dispersion relation of this mode is independent of T and its damping rate is not quantized but varies as T^{-3} or T^{-2}. It can be distinguished from the fundamental EMP due to its specific properties like the strong charge oscillations transverse to the edge.
(c) As regards the behaviour of the charge-density amplitudes of the low-frequency edge helicon, we remark that the convergence shown in the imaginary part of the density profile $\delta\rho_i$ (figures 4 and 6) is substantially slower than that of the corresponding real part $\delta\rho_r$ (figures 3 and 5), for the reasons pointed out in section 3.1. Here, we just mention that this behaviour is related to the absence of the lowest term (monopole) in the expansion of $\delta\rho_i$, while it is present in $\delta\rho_r$.

For $\nu = 4$, the modes of the $n = 1$ LL were studied in the regimes of weak and strong dissipation. It was shown that the fundamental mode of the $n = 1$ LL, decoupled from the excitations of the $n = 0$ LL, is very weakly damped even for strong dissipation. On the other hand, when the inter-LL Coulomb coupling with the $n = 0$ LL fundamental EMP is turned on, the dispersion relations of the two fundamental modes change drastically, leading to a renormalization of the fundamental modes of the $n = 0$ LL and $n = 1$ LL. We must emphasize that, as was shown in figure 3 of reference [3], the dispersion relations of these

renormalized fundamental modes describe the spectrum of modes found experimentally quite well (see figure 3(a) of reference [4]).

We have neglected the spin splitting for even ν. Though this is a reasonable approximation for the bulk of the channel, its validity near the edges cannot be guaranteed, in view of the work of references [20] and [21].

Acknowledgments

This work was supported by Brazilian FAPESP Grants No 98/10192-2 and No 95/0789-3 and Canadian NSERC Grant No OGP0121756. In addition, OGB acknowledges partial support by the Ukrainian SFFI Grant No 2.4/665 and NS is grateful to the Brazilian CNPq for a research fellowship.

References

[1] Volkov V A and Mikhailov S A 1988 *Zh. Eksp. Teor. Fiz.* **94** 217 (Engl. Transl. 1988 *Sov. Phys.–JETP* **67** 1639)
[2] Aleiner I L and Glazman L I 1994 *Phys. Rev. Lett.* **72** 2935
[3] Balev O G and Vasilopoulos P 1998 *Phys. Rev. Lett.* **81** 1481
[4] Ernst G, Haug R J, Kuhl J, von Klitzing K and Eberl K 1996 *Phys. Rev. Lett.* **77** 4245
[5] Kelvin W T 1880 *Phil. Mag.* **x** 97
[6] Tal'yanskii V I, Wassermeier M, Wixforth A, Oshinowo J, Kotthaus J P, Batov I E, Weinmann G, Nikel H and Schlapp W 1990 *Surf. Sci.* **229** 40
[7] Wassermeier M, Oshinowo J, Kotthaus J P, MacDonald A H, Foxon C T and Harris J J 1990 *Phys. Rev.* B **41** 10 287
[8] Ashoori R C, Stormer H L, Pfeiffer L N, Baldwin K W and West K 1992 *Phys. Rev.* B **45** 3894
[9] Wen X G 1991 *Phys. Rev.* B **43** 11 025
Stone M 1991 *Ann. Phys., NY* **207** 38
[10] Giovanazzi S, Pitaevskii L and Stringari S 1994 *Phys. Rev. Lett.* **72** 3230
Palacios J J and MacDonald A H 1996 *Phys. Rev. Lett.* **76** 118
[11] Stone M, Wyld H W and Shult R L 1992 *Phys. Rev.* B **45** 14 156
de Chamon C and Wen X G 1994 *Phys. Rev.* B **49** 8227
Zulicke U and MacDonald A H 1996 *Phys. Rev.* B **54** 16 813
[12] Balev O G and Vasilopoulos P 1993 *Phys. Rev.* B **47** 16 410
Balev O G and Vasilopoulos P 1994 *Phys. Rev.* B **50** 8706
Balev O G and Vasilopoulos P 1994 *Phys. Rev.* B **50** 8727
[13] Balev O G and Vasilopoulos P 1996 *Phys. Rev.* B **54** 4863
[14] Chklovskii D B, Shklovskii B I and Glazman L I 1992 *Phys. Rev.* B **46** 4026
[15] Suzuki T and Ando T 1993 *J. Phys. Soc. Japan* **62** 2986
[16] Brey L, Palacios J J and Tejedor C 1993 *Phys. Rev.* B **47** 13 884
[17] Balev O G and Vasilopoulos P 1997 *Phys. Rev.* B **56** 13 252
[18] Balev O G and Vasilopoulos P 1999 *Phys. Rev.* B **59** 2807
Balev O G, Vasilopoulos P and Studart N 1999 *Proc. 24th Int. Conf. on the Physics of Semiconductors* (Jerusalem: World Scientific)
[19] Muller G, Weiss D, Khaetskii A V, von Klitzing K, Koch S, Nickel H, Schlapp W and Losch R 1992 *Phys. Rev.* B **45** 3932
[20] Dempsey J, Gelfand B Y and Halperin B I 1993 *Phys. Rev. Lett.* **70** 3639
[21] Balev O G and Vasilopoulos P 1997 *Phys. Rev.* B **56** 6748